

Influence of Input Image Size Variations and Data Balancing on VGG-16 and VGG-16-ELM Models for Pneumonia Classification

Mohammad Agil Rofiqul Zein^{1*}, Basuki Rahmat², Eva Yulia Puspaningrum³

^{1,2,3} Universitas Pembangunan Nasional Veteran Jawa Timur
mohammadagilrz11@gmail.com^{1*}

Abstract

Pneumonia is a lung disease that can be identified through chest X-ray images. This study aims to evaluate the performance of two deep learning models, namely VGG-16 and a combination of VGG-16 with Extreme Learning Machine (ELM), in automatically classifying pneumonia. The approach used includes an analysis of variations in input image sizes (150×150, 200×200, 224×224, 256×256, and 300×300 pixels) as well as the application of data balancing techniques using Random Over Sampling (ROS). The dataset used contains 5,856 X-ray images classified into two classes: NORMAL and PNEUMONIA. The preprocessing stages include resizing, normalization, data splitting, and augmentation. Performance evaluation is conducted using metrics of accuracy, precision, recall, and F1-score. The experimental results show that the input size of 200×200 consistently yields the best performance. The VGG-16 model without the application of ROS achieved the highest accuracy of 96.59% and an F1-score of 97.69%. Meanwhile, the VGG-16-ELM combination showed significant performance improvement when ROS was applied. These findings indicate that the selection of model architecture, data balancing techniques, and input image size significantly influence classification accuracy, and contribute to the development of AI-based automated diagnostic systems.

Keywords: Pneumonia, Deep Learning, VGG-16, Extreme Learning Machine, Data Balancing.

1. Introduction

The lungs are vital organs in the respiratory and circulatory systems that function in gas exchange, namely expelling carbon dioxide from the blood into the air[1]. This system is very vulnerable to disturbances caused by infections, air pollution, unhealthy lifestyles, and other environmental factors. Diseases such as asthma, bronchitis, and pneumonia are common disorders that affect lung function, where air quality is one of the significant external factors (World Health Organization, "Air pollution and health", 2021). Pneumonia is inflammation of the lung tissue caused by bacterial, viral, fungal, or parasitic infections and can be fatal if not properly managed[2]. According to BPJS Kesehatan data from 2023, pneumonia is the disease with the highest cost burden, amounting to Rp8.7 trillion (Ministry of Health of the Republic of Indonesia, "Pneumonia Continues to Threaten Children", 2024).

Technological advancements have enabled the utilization of artificial intelligence, particularly in medical image analysis, to support the diagnostic process. Convolutional Neural Network (CNN) is one of the widely used methods due to its ability to automatically extract complex features from images. CNN architectures like VGG-16 have proven effective in medical image classification tasks, including pneumonia detection[3]. VGG-16 is a CNN architecture that consists of 16 parameterized layers with small filters (3×3) capable of capturing detail in images. This architecture is often used due to its ability to preserve important information while simplifying data representation[4]. In a study by Candra et al. (2024), the pre-trained VGG-16 achieved 97% accuracy in detecting brain tumors through MRI images with the support of data augmentation[5].

To improve performance, VGG-16 can be combined with the Extreme Learning Machine (ELM) algorithm, which is known for its high training speed. The CNN-ELM combination has proven to outperform conventional CNNs in various image input sizes[6]. ELM also offers high efficiency in health data classification[7]. Besides architecture, the size of the input image and data balance also affect model accuracy. Studies show that image sizes of 200×200 [6], 224×224 [8], and 256×256 [5] provide high performance depending on the scenario. In addition, the use of the Random Over Sampling (ROS) method to balance the data has been shown to significantly improve model accuracy [9].

This study aims to analyze the effect of variations in image input size and data balancing on the performance of the VGG-16 and VGG-16-ELM models in classifying pneumonia based on chest X-ray images. The dataset used was obtained from Kaggle and includes images

of normal lungs as well as pneumonia. An easy way to comply with the paper formatting requirements is to use this document as a template and simply type your text into it.

2. Literature Review

2.1. Deep Learning

Deep Learning is a branch of machine learning that utilizes multi-layer artificial neural network architecture to learn hierarchical data representations. This architecture is designed to resemble the workings of the human brain, where neuron units are interconnected to form a complex network. The term Deep Learning is also often referred to as deep structured learning, hierarchical learning, or deep neural networks. This method employs a series of layered non-linear transformations to automatically extract features from input data. This approach represents a combination of machine learning techniques and the concept of artificial neural networks[6]. Some algorithms that fall under the category of Deep Learning include Convolutional Neural Networks (CNN), Restricted Boltzmann Machines (RBM), Deep Belief Networks (DBN), and Stacked Autoencoders[6].

2.2. Convolutional Neural Network

Convolutional Neural Network (CNN) is a supervised learning algorithm specifically designed for processing two-dimensional (2D) image data, making it very effective for digital image recognition tasks. CNN is developed from the Multi Layer Perceptron (MLP) architecture and is widely used in various deep learning applications. Some popular CNN architectures include VGG-16, ResNet, AlexNet, GoogLeNet, and MobileNet [10].

In general, image data processing in CNN consists of two main stages: feature learning and classification. In the feature learning stage, CNN automatically extracts important features from images through convolutional layers, the ReLU activation function, and pooling which serves to reduce the spatial dimensions of the features. The classification stage then utilizes these features through flatten and fully connected layers, with a softmax function at the end to determine the output class probabilities[10]. An illustration of the CNN architecture is shown in Figure 1.

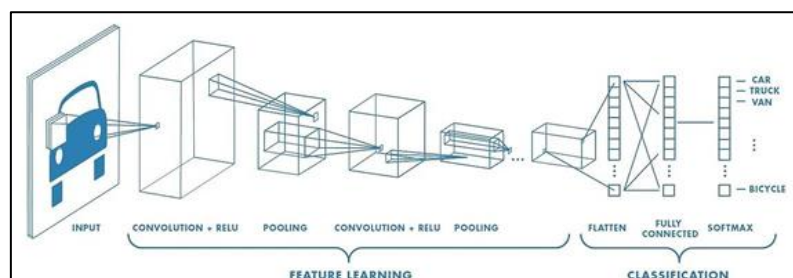


Figure 1: Convolutional Neural Networks [10]

2.3. Extreme Learning Machine

Extreme Learning Machine (ELM) is a learning method on Artificial Neural Networks (ANN) developed from the feedforward architecture. ELM uses a Single Hidden Layer Feedforward Neural Networks (SLFNs) structure with a design similar to conventional ANN, but it is designed to improve training efficiency. This method was introduced as a solution to the limitations of training speed on traditional ANN[11]. According to Huang and colleagues, there are two main factors that cause slow training in conventional feedforward ANN:

1. The use of gradient-based algorithms that take a long time to converge.
2. The parameter computation process is done iteratively for all weights in the network.

ELM addresses this issue by randomly assigning input weights and biases, and calculating output weights analytically without an iterative process[11]. The basic structure of the ELM method is shown in Figure 2.

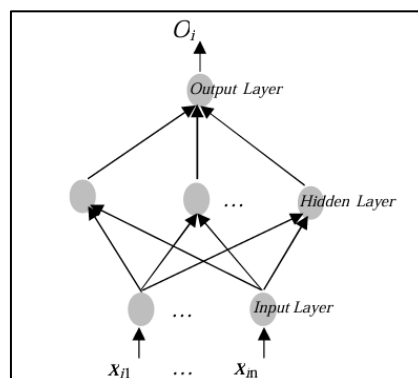


Figure 2: ELM Structure [11]

2.4. VGG-16

VGG-16 is an extension of the AlexNet architecture with the main difference being the use of small convolution kernels, specifically 3×3 . This model has 13 convolutional layers and 3 fully connected layers, with a total of about 138 million parameters [12]. Its architecture also includes 5 max pooling layers, and utilizes ReLU and softmax activation functions at the final stage [13].

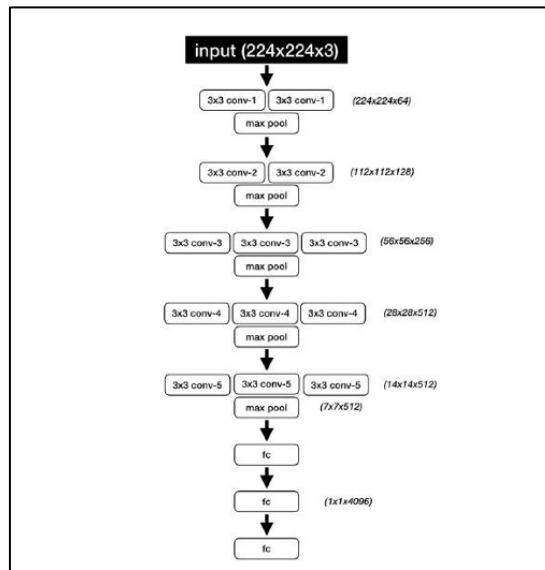


Figure 3: VGG-16 Model Architecture [13]

As shown in Figure 3 VGG-16 receives input in the form of images sized 224×224 pixels with 3 color channels. The initial layers use 64 filters, followed by layers with 128, 256, and two times 512 filters, each accompanied by ReLU activation and max pooling. Three fully connected layers and one output layer form the final classification stage in this architecture [14].

2.5. Variations of Image Input Size

The size of the input image has a significant impact on the performance of the classification model. Research by [15] shows that variations in image size can affect the accuracy of CNN models in detecting pneumonia, where certain sizes yield more optimal classification results [6]. In the preprocessing stage, interpolation techniques play an important role, especially when adjusting the dimensions of images to meet the needs of deep learning architectures. One well-known interpolation method that produces high-quality images is the LANCZOS method. This method uses a modified sinc function to calculate pixel values based on contributions from neighboring pixels, thus better preserving visual details compared to other methods such as nearest neighbor or bilinear [15].

2.6. Balancing Data

Data imbalance is one of the common problems in machine learning that can decrease model performance, especially on evaluation metrics such as precision, recall, and F1-score. This condition occurs when the distribution between classes is not balanced, causing the model to be biased toward the majority class [16]. To address this problem, various balancing techniques have been developed, both through undersampling (e.g., Tomek Links, Cluster Centroids) and oversampling (such as Borderline-SMOTE), which have been shown to improve model performance on imbalanced datasets. Among the most commonly used techniques are Random Oversampling (ROS) and Random Undersampling (RUS). ROS works by duplicating samples from the minority class until it is balanced with the majority class, while RUS reduces the number of samples from the majority class to match the minority class count [9].

3. Research Methods

This research aims to design a pneumonia classification system by utilizing the VGG-16 architecture and a combination of VGG-16 with Extreme Learning Machine (ELM). In addition, this research also aims to evaluate the impact of variations in image input sizes and data balancing techniques on the performance of the developed model. The research process is conducted through several main stages, namely

data collection, image preprocessing, model architecture design, training, as well as testing and evaluation. Overall, the flow of this research is illustrated in the diagram in Figure 4.

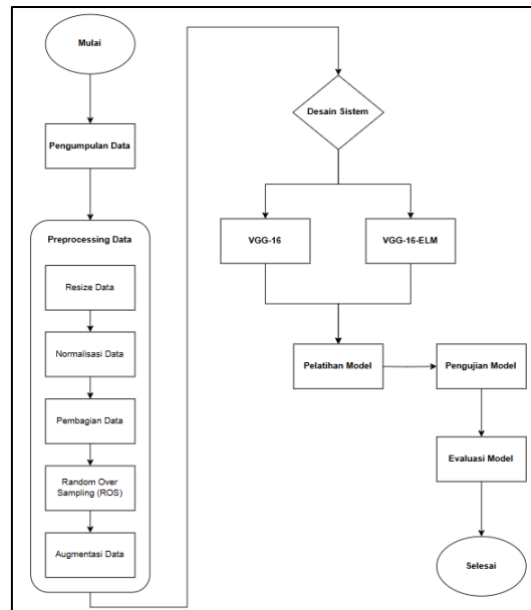


Figure 4: Research Methodology

3.1. Data Collection

In the data collection stage, the dataset used was obtained from open sources available on the Kaggle platform, consisting of (Chest X-ray Images). After the downloading process, the data was organized into folders based on class categories and prepared for the next processing stage. This dataset consists of a total of 5,856 JPEG formatted images, divided into two main classes, namely 1,583 images of normal lungs and 4,273 images of lungs diagnosed with pneumonia. All images have an average resolution of about 1000×1000 pixels. The dataset is shown in Figure 5.

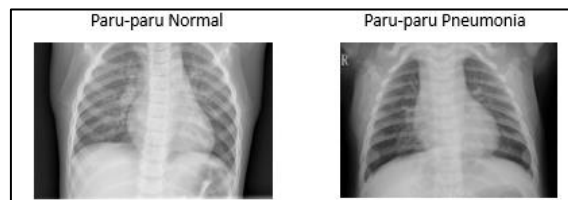


Figure 5: Chest X-ray Data

3.2. Preprocessing Data

The data preprocessing stage is carried out to prepare the images before the model training process. There are five main steps in this stage:

1. **Resize Data:** The original X-ray images, which were larger than 1000×1000 pixels, are resized into five variations of resolutions: 150×150, 200×200, 224×224, 256×256, and 300×300 pixels, according to the testing scenarios.
2. **Normalize Data:** All pixel values are normalized into the range [0–1] by dividing each pixel value by 255. This step aims to accelerate the convergence process during model training.
3. **Data Splitting:** The dataset, consisting of 5,856 images, is divided into three subsets: 80% training data (4,685 images), 10% validation data (586 images), and 10% testing data (586 images). The splitting results show an imbalance in the distribution between the NORMAL and PNEUMONIA classes, particularly in the training data subset.
4. **Random Oversampling (ROS):** To address class imbalance, the ROS technique is used by adding duplicate data to the minority class (NORMAL) until its number is equal to that of the majority class (PNEUMONIA).
5. **Data Augmentation:** To increase the diversity of the training data and prevent overfitting, image augmentation techniques such as zooming, flipping, and rotating are applied. This step helps the model to achieve better generalization to new data.

3.3. System Design

This research aims to develop a medical image classification model using the VGG-16 architecture and its combination with Extreme Learning Machine (ELM). Two scenarios were tested:

1. VGG-16 was used in its entirety for feature extraction and classification.
2. A combination of VGG-16 as a feature extractor with ELM as the classifier.

The research also analyzes the impact of varying input image sizes and the application of Random Over Sampling (ROS) to address data imbalance. This approach is expected to produce an optimal pneumonia classification model in each scenario.

3.4. Model Training

At this stage, the training process is carried out using training data that has undergone preprocessing stages. The data is then processed using two model algorithms, namely VGG-16 and VGG-16-ELM. During training, several important parameters are used such as batch size, epoch, learning rate, dropout, and other parameters that are adjusted to the needs of the model. The arrangement of these parameters aims to support effectiveness and optimize the model's performance during the training process.

3.5. Model Testing

The testing process was conducted using 586 test data samples, consisting of 158 normal labeled images and 427 pneumonia labeled images. At this stage, the trained model is evaluated to measure its ability to classify chest X-ray images into these two categories. The model's performance evaluation is carried out using accuracy, precision, recall, and F1-score metrics to assess how effectively the model can recognize each class.

3.6. Model Evaluation

The model evaluation process is carried out through several stages. First, the trained model is used to classify the test data, generating class predictions based on input images. The prediction results are then analyzed using a confusion matrix to evaluate the number of correct and incorrect predictions. Furthermore, the model's performance is assessed based on metrics such as accuracy, precision, recall, and F1-score to identify the model with the most optimal results. This evaluation provides a comprehensive overview of the model's ability to produce accurate and balanced predictions, as well as supports the selection of the best model to be applied in pneumonia classification.

4. Results and Discussion

The model training was conducted for a total of ten scenarios for the VGG-16 model and ten scenarios for the VGG-16-ELM model, varying the input image sizes of (150×150, 200×200, 224×224, 256×256, and 300×300 pixels), as well as using the ROS technique and without the ROS technique. Below is one of the results of the training and testing from all research scenarios.

4.1. Model Training Results

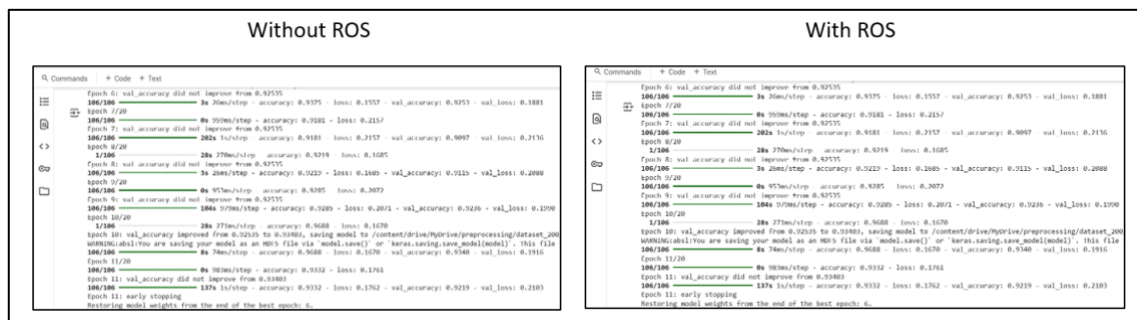


Figure 6: Training Results of 200x200 VGG-16

Figure 6 shows the training results of the VGG-16 model with 200x200 pixels without the use of ROS (Random Over Sampling) and with ROS. In the scenario without ROS, the highest validation accuracy reached 95.31%, while with the use of ROS, the validation accuracy reached 92.53%.



Figure 7: Training Results of 200x200 VGG-16-ELM

Figure 7 shows the training results of the VGG-16-ELM model with 200x200 pixels without the use of ROS (Random Over Sampling) and with ROS. In the scenario without ROS, the highest validation accuracy reached 93.50%, while with the use of ROS, the validation accuracy reached 93.33%.

4.2. Model Testing Results

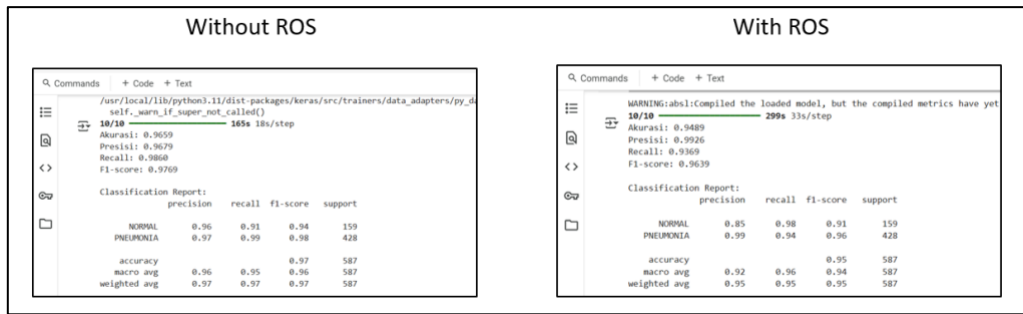


Figure 8: Testing Results of 200x200 VGG-16

Figure 8 shows the testing results of the VGG-16 model with 200x200 pixels without the use of ROS (Random Over Sampling) and with ROS. In the without ROS scenario, the classification report shows that the NORMAL class achieved a recall value of 0.91, while the PNEUMONIA class achieved a recall value of 0.99. In the with ROS scenario, the NORMAL class obtained a higher recall value of 0.98, while the PNEUMONIA class had a slightly lower recall value of 0.94. The recall value reflects the model’s ability to correctly identify instances of each class.

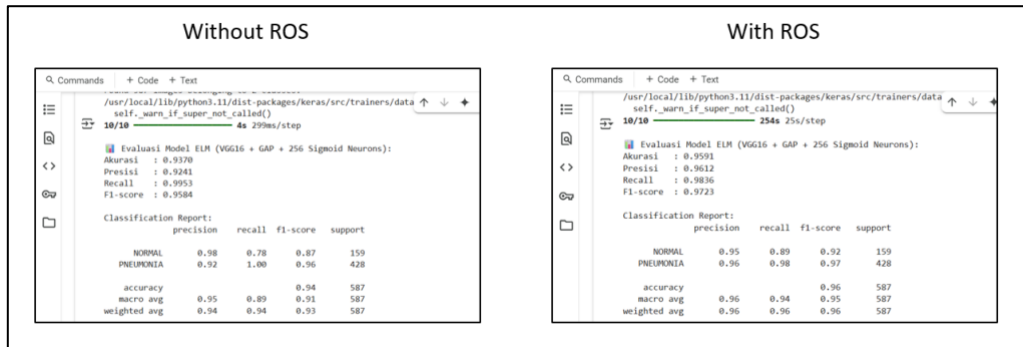


Figure 9: Testing Results of 200x200 VGG-16-ELM

Figure 9 shows the testing results of the VGG-16-ELM model with 200x200 pixels without the use of ROS (Random Over Sampling) and with ROS. In the without ROS scenario, the classification report shows that the NORMAL class achieved a recall value of 0.78, while the PNEUMONIA class achieved a recall value of 1.00. In the with ROS scenario, the NORMAL class achieved a recall value of 0.89, while the PNEUMONIA class achieved a recall value of 0.98. The recall value reflects the model’s ability to correctly identify instances of each class.

4.3. Confusion Matrix Results

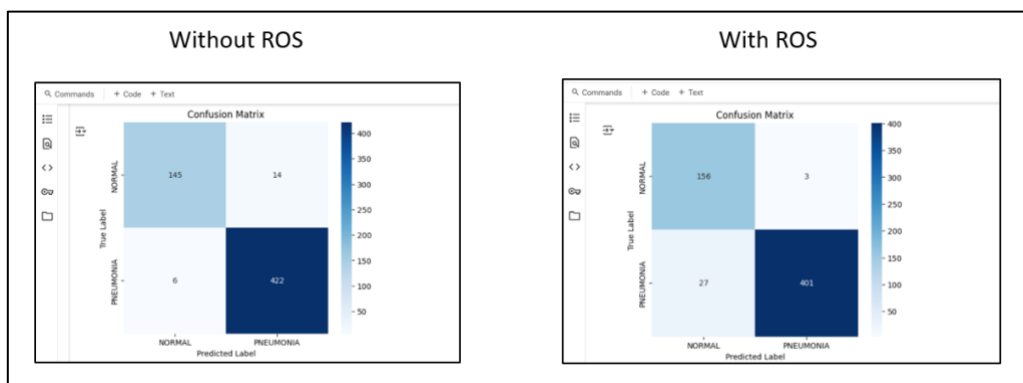


Figure 10: Confusion Matrix Results of 200x200 VGG-16

Figure 10 shows the confusion matrix results of the VGG-16 model with 200x200 pixels without the use of ROS (Random Over Sampling) and with ROS. In the scenario without ROS, the model makes fewer mistakes in classifying the PNEUMONIA class with a correct count of 422, whereas in the scenario with ROS, the model makes more mistakes in classifying the PNEUMONIA class with a correct count of 401.

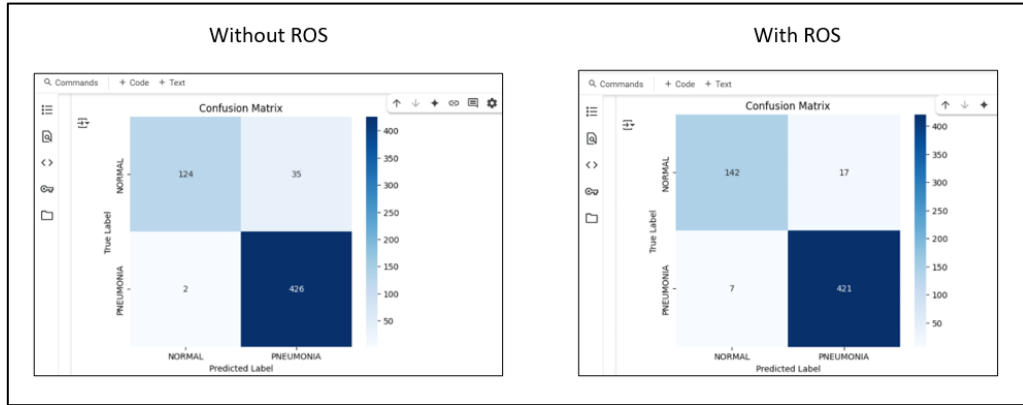


Figure 11: Confusion Matrix Results of 200x200 VGG-16-ELM

Figure 11 shows the confusion matrix results of the VGG-16-ELM model with 200x200 pixels without the use of ROS (Random Over Sampling) and with ROS. In the scenario without ROS, the model makes fewer mistakes in classifying the PNEUMONIA class with a correct count of 426, whereas in the scenario with ROS, the model makes more mistakes in classifying the PNEUMONIA class with a correct count of 421.

4.4. Research Scenario Results

Table 1: Research Scenario Results

No	Model	Input Variation	Balancing Data	Accuracy	Precision	Recall	F1-Score
1	VGG-16	150×150	Without Balancing Data	0.9267	0.9800	0.9182	0.9481
		200×200		0.9659	0.9679	0.9860	0.9769
		224×224		0.9625	0.9788	0.9696	0.9742
		256×256		0.9574	0.9879	0.9533	0.9703
		300×300		0.9302	0.9329	0.9743	0.9531
2	VGG-16	150×150	ROS	0.9250	0.9800	0.9159	0.9469
		200×200		0.9489	0.9926	0.9369	0.9639
		224×224		0.9336	0.9949	0.9136	0.9525
		256×256		0.9302	0.9899	0.9136	0.9502
		300×300		0.9250	0.9848	0.9112	0.9466
3	VGG-16-ELM	150×150	Without Balancing Data	0.9131	0.9107	0.9766	0.9425
		200×200		0.9370	0.9241	0.9953	0.9584
		224×224		0.9029	0.8989	0.9766	0.9362
		256×256		0.9165	0.9165	0.9743	0.9445
		300×300		0.9284	0.9347	0.9696	0.9518
4	VGG-16-ELM	150×150	ROS	0.9114	0.9332	0.9463	0.9397
		200×200		0.9591	0.9612	0.9836	0.9723
		224×224		0.9455	0.9583	0.9673	0.9628
		256×256		0.9489	0.9650	0.9650	0.9650
		300×300		0.9336	0.9576	0.9509	0.9543

Based on Table 1 the VGG-16 model without data balancing with an input size of 200×200 provides the best performance with an accuracy of 96.59%, precision of 0.9679, recall of 0.9860, and F1-Score of 0.9769. The application of data balancing using the Random Over Sampling (ROS) method tends to decrease the model's performance, especially at input sizes of 150×150 and 300×300. Meanwhile, the VGG-16-ELM model shows improved performance with data balancing, particularly at an input size of 200×200, yielding an accuracy of

95.91%, recall of 98.36%, and F1-Score of 0.9723. Overall, although data balancing has a positive impact on VGG-16-ELM, the best performance is still achieved by the VGG-16 model without data balancing at an input size of 200×200.

4.5. Testing Graph

This section presents a comparison graph of accuracy values for all scenario tests on the VGG-16 and VGG-16-ELM model.

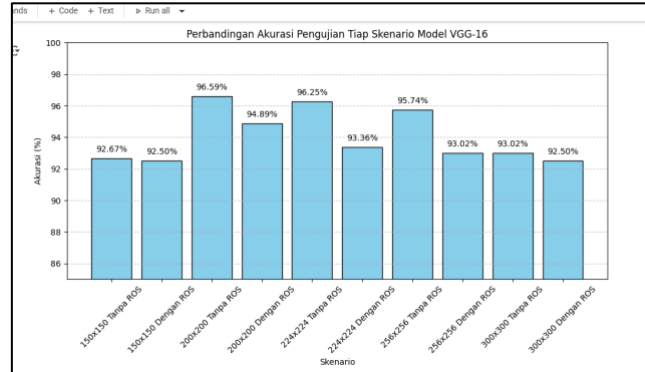


Figure 12: VGG-16 Model Testing Graph

Figure 12 shows the accuracy comparison of the VGG-16 model across various testing scenarios. The highest accuracy was achieved in the 200×200 scenario without ROS at 96.59%, followed by 224×224 and 256×256 scenarios without ROS with accuracies of 96.25% and 95.74% respectively. The lowest accuracy was recorded in the 150×150 and 300×300 scenarios with ROS at 92.50%. Overall, the model demonstrated stable performance with accuracy above 93% in most scenarios. The 200×200 size without ROS emerged as the most optimal configuration, while the use of ROS did not always enhance accuracy.

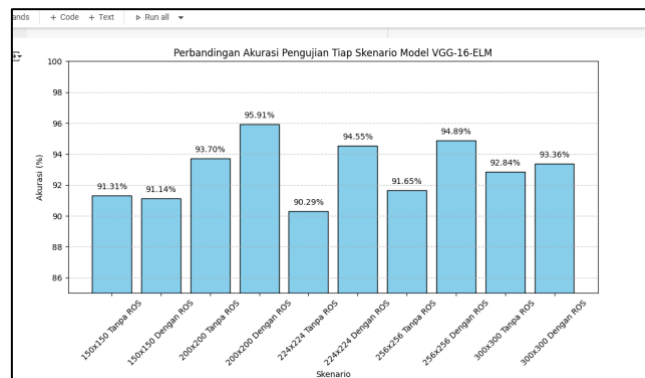


Figure 13: VGG-16-ELM Model Testing Graph

Figure 13 shows a comparison of the accuracy of the VGG-16-ELM model under various scenarios. The highest accuracy was achieved in the 200×200 scenario with a ROS of 95.91%, followed by 256×256 and 224×224 with ROS, showing an accuracy of 90.29%. Overall, the application of ROS proved to improve accuracy, demonstrating the effectiveness of data balancing in reducing class bias. Additionally, the size of the input image also influenced the results, with 200×200 being the most optimal configuration. These findings emphasize the importance of selecting image sizes and balancing techniques to optimize model performance.

5. Conclusion

In this study, a comprehensive evaluation of the VGG-16 and VGG-16-ELM models was conducted based on variations in input image size and the application of Random Over Sampling (ROS) for data balancing in the classification of pneumonia from chest X-ray images. The results demonstrate that input image size significantly influences model performance, with the 200×200 pixel configuration consistently yielding the highest accuracy and F1-Score across both models. A key finding is that data balancing with ROS had contrasting effects: it reduced performance in the baseline VGG-16 model but improved it in the hybrid VGG-16-ELM model. Notably, the best overall performance was achieved by the VGG-16 model without balancing data, reaching an accuracy of 96.59% and F1-Score of 0.9769. These findings highlight the importance of input dimension selection and model-balancing strategy alignment, and further demonstrate that while hybrid approaches like VGG-16-ELM can benefit from oversampling, conventional CNN architectures may achieve optimal results without it.

Acknowledgement

The author expresses the deepest gratitude to the supervising lecturers for all the guidance, direction, and motivation given during the research process. Thanks also go to the beloved family for their prayers, support, and unwavering spirit. Lastly, the author appreciates the fellow companions who continuously provided support and encouragement during the preparation of this research.

References

- [1] F. Antony, H. Irsyad, and M. E. Al Rivan, "KNN and Gabor Filter as well as Wiener Filter for Diagnosing Pneumonia in X-RAY Images of the Lungs," *J. Algoritm.*, vol. 1, no. 2, pp. 147–155, 2021, doi: 10.35957/algoritme.v1i2.893.
- [2] R. A. Wati, H. Irsyad, and M. E. A. R. Rivan, "Pneumonia Classification Using Support Vector Machine Method," *J. Algoritm.*, vol. 1, no. 1, pp. 21–32, 2020, [Online]. Available: <http://download.garuda.kemdikbud.go.id/article.php?article=2652619&val=24585&title=PNEUMONIA CLASSIFICATION USING SUPPORT VECTOR MACHINE>.
- [3] T. Berliani, E. Rahardja, and L. Septiana, "Comparison of X-ray Lung Image Classification Ability Using Transfer Learning ResNet-50 and VGG-16," *J. Med. Heal.*, vol. 5, no. 2, pp. 123–135, 2023, doi: 10.28932/jmh.v5i2.6116.
- [4] M. A. Ridho and M. Arman, "Analysis of DDoS Attacks Using Artificial Neural Network Method," *J. Sisfokom (Information Systems and Computer)*, vol. 9, no. 3, pp. 373–379, 2020, doi: 10.32736/sisfokom.v9i3.945.
- [5] D. Candra, G. Wibisono, M. Ayu, and M. Afrad, "Transfer Learning Convolutional Neural Network model using VGG-16 for Brain Tumor Classification on MRI Images," *LEDGER J. Inform. Inf. Technol.*, vol. 3, no. 1, pp. 11–18, 2024.
- [6] B. Nugroho and E. Y. Puspaningrum, "Performance of CNN Method for Pneumonia Classification with Variations in Input Image Sizes," *J. Teknol. Inf. dan Ilmu Komput.*, vol. 8, no. 3, pp. 533–538, 2021, doi: 10.25126/jtiik.2021834515.
- [7] V. V. Nurdiansyah, I. Cholissodin, and P. P. Adikara, "Tuberculosis (TB) Disease Classification using Extreme Learning Machine (ELM) Method," *J. Pengemb. Teknol. Inf. dan Ilmu Komput.*, vol. 4, no. 5, pp. 1387–1393, 2020.
- [8] S. A. Suryaman, R. Magdalena, and S. Sa'idah, "Weather Classification Using VGG-16 Method, Principal Component Analysis, and K-Nearest Neighbor," *J. Ilmu Komput. dan Inform.*, vol. 1, no. 1, pp. 1–8, 2021, doi: 10.54082/jiki.1.
- [9] M. Harits, R. Ramadhan, and Y. Miftahuddin, "The Effect of Data Balancing on Pneumonia Classification Using VGG16," pp. 1–11, 2023.
- [10] S. N. Nugraha, R. Pebrianto, and E. Fitri, "Application of Deep Learning in the Classification of Paprika Plants Based on Leaf Images Using the CNN Method," *Inf. Syst. Educ. Prof. J. Inf. Syst.*, vol. 8, no. 2, p. 15, 2023, doi: 10.51211/isbi.v8i2.2671.
- [11] P. P. Winangun, I. M. O. Widyantara, and R. S. Hartati, "A Diagnostic Approach Based on Extreme Learning Machine with Linear Kernel to Classify Lung Abnormalities," *Maj. Ilm. Teknol. Elektro*, vol. 19, no. 1, p. 83, 2020, doi: 10.24843/mite.2020.v19i01.p12.
- [12] L. Listyalina et al., "Determination of Lung Diseases Using Artificial Neural Networks," *J. SIMETRIS*, vol. 11, no. 1, pp. 233–240, 2020.
- [13] R. AGUSTINA, R. MAGDALENA, and N. K. C. PRATIWI, "Classification of Skin Cancer using Convolutional Neural Network Method with VGG-16 Architecture," *ELKOMIKA J. Technol. Electr. Energy*, vol. 10, no. 2, p. 446, 2022, doi: 10.26760/elkomika.v10i2.446.
- [14] W. Swastika, "Preliminary Study on COVID-19 Detection Using CT Images Based on Deep Learning," *J. Technol. Inf. and Computer Science*, vol. 7, no. 3, pp. 629–634, 2020, doi: 10.25126/jtiik.2020733399.
- [15] S. Fadnavis, "Image Interpolation Techniques in Digital Image Processing: An Overview," *J. Eng. Res. Appl.* www.ijera.com, vol. 4, no. November 2014, pp. 70–73, 2014, [Online]. Available: www.ijera.com.
- [16] R. Mohammed, J. Rawashdeh, and M. Abdullah, "Machine Learning with Oversampling and Undersampling Techniques: Overview Study and Experimental Results," 2020 11th Int. Conf. Info. Commun. Syst. ICICS 2020, pp. 243–248, 2020, doi: 10.1109/ICICS49469.2020.239556.
- [17] World Health Organization, 'Air pollution and health,' 2021.
- [18] Ministry of Health of the Republic of Indonesia, 'Pneumonia Continues to Threaten Children,' Ministry of Health RI, November 18, 2024.